Liquid Distribution and RTD in Trickle Bed Reactors: Experiments and CFD Simulations

Prashant R. Gunjal, Vivek V. Ranade* and Raghunath .V. Chaudhari

Industrial Flow Modeling Group, Homogeneous Catalysis Division National Chemical Laboratory, Pune 411008

Hydrodynamics and mixing in trickle bed reactors (TBR) are governed by bed porosity, capillary forces, wetting and non-uniform distribution at the inlet. In this work, experiments were carried out to study pressure drop, liquid hold-up and residence time distribution for pre-wetted and non-wetted bed. CFD models were developed, in which bed heterogeneity and capillary models were incorporated. Mixing and RTD were simulated using the CFD model. This study was further extended to study the flow mal-distribution in TBR. Based on these results, current capabilities and limitations of the CFD model were discussed. The model and the results discussed here would be useful to extend application of CFD models for simulating mixing in TBR.

L'hydrodynamique et le mélange dans les réacteurs à lits ruisselants (TBR) sont gouvernés par la porosité du lit, les forces capillaires, le mouillage et la distribution non uniforme à l'entrée. Dans ce travail, on a mené des expériences afin d'étudier la perte de charge, la rétention de liquide et la distribution de temps de séjour pour des lits pré-mouillés et non mouillés. Des modèles de CFD ont été mis au point, dans lesquels l'hétérogénéité des lits et des modèles capillaires sont introduits. Le mélange et la RTD ont été simulés à l'aide du modèle de CFD. Cette étude a été généralisée pour étudier la mauvaise distribution de l'écoulement en TBR. D'après ces résultats, les capacités et limites actuelles du modèle de CFD sont examinées. Le modèle et les résultats analysés ici pourraient être utiles pour étendre l'application des modèles de CFD à la simulation du mélange en TBR.

Keywords: trickle bed reactor, CFD, mixing, RTD and flow mal-distribution.

Liquid flow distribution and mixing are key parameters for designing of trickle bed reactors. Residence time distribution (RTD) was used for many years to analyze and characterize the flow non-idealities and mixing because of the un-availability of detailed flow information inside the reactor. RTD in trickle bed reactor (TBR) is a useful tool to understand many aspects of the reactor such as kinetic processes (Ramachandra and Smith, 1987), wetting characteristics (Schwartz et al., 1976), channeling (Oliveros et al.,1982), flow maldistribution (Hanratty and Dudukovic, 1992) and liquid mixing (Higler et al., 1999; Gulijk, 1998). Hydrodynamics and mixing in trickle bed reactors are governed by several factors including non-uniform porosity distribution of the bed, capillary forces, wetting and non-uniform distribution of flow at the inlet. Large variation in hydrodynamic parameters such as pressure drop, liquid hold-up and liquid distribution have been observed for pre-wetted bed and non-wetted bed (Szady and Sundaresan, 1991). Conventional modeling approach uses uniform porosity and velocity through the bed and lump all the non-idealities in flow and mixing in dispersion coefficient. Tracer experiments are carried out in TBR and the dispersion coefficient is fitted based on outlet tracer response, which is expected to represent complex flow, mixing, wetting, channeling, stagnancy and dead zones in TBR. Extrapolation based on such lumped models is uncertain and often inadequate for design purposes.

Computational fluid dynamics (CFD) based models have recently been applied to simulate flow in TBR (Jiang et al. 2002; Ranade et al. 2002). In this work, we extend the CFD models to simulate and to understand hydrodynamics and RTD in trickle bed reactors. The objective of the work was to understand the flow non-idealities and contribution of various parameters, such as bed heterogeneity, capillarity, flow distribution using computational fluid dynamics and tracer residence time distribution in trickle bed reactor. For this purpose, experiments were carried out to study the hydrodynamic parameters, such as pressure drop and liquid hold-up, for complete wetting and non-wetting conditions at different operating conditions. Tracer was injected inside the bed and outlet response was measured. Experiments were carried for uniform and non-uniform inlet conditions. Comprehensive two-dimensional and three-dimensional CFD models were developed, in which bed heterogeneity and capillary models were incorporated. Mixing and tracer residence time distribution was simulated using the CFD model. Simulated results were compared with experimental data. Experiments, as well as model predictions, showed interesting results for non-wetted and pre-wetted bed conditions. The current capabilities and limitations of the CFD model were also pointed out with the help of experimental and simulation results obtained for the non-uniform liquid inlet. The model and the results discussed here would be useful to extend application of CFD models for simulating mixing in TBR.

*Author to whom correspondence may be addressed. E-mail address: vvranade@ifmg.ncl.res.in

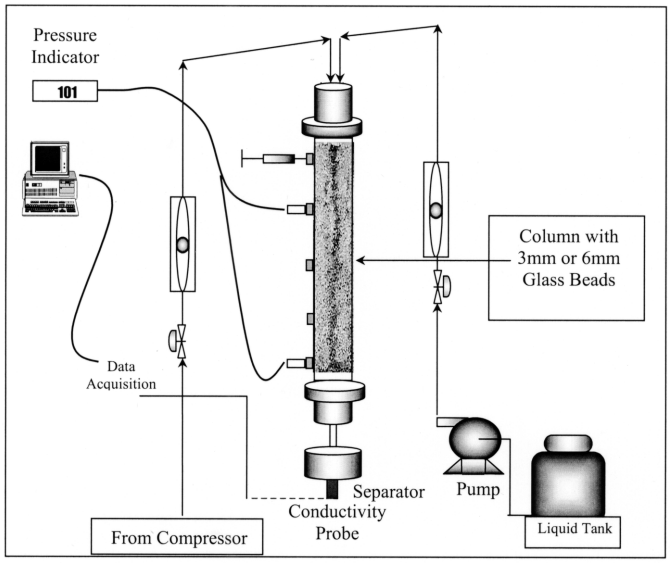

Figure 1. Experimental set-up of trickle bed reactor for hydrodynamics and RTD study.

Experimental

Set-up

Trickle bed reactor (Perspex) of 0.1 m diameter and 1 m height was set-up for experimental study. The schematic of experimental set-up is shown in Figure 1. Gas and liquid were introduced in the column at the top. Gas and liquid flow rates were measured with the calibrated rotameters. The distributor plate was made up of stainless steel with uniform 3mm holes, which were arranged in triangular pitch of 3 mm. Glass beads either of 3 mm or 6 mm diameter were filled in the column such that beads are placed compactly in the column. Voidage of the column was measured using liquid drainage method. The measured voidage of the columns were found to be 0.37 for 3 mm particle and 0.356 for 6 mm particles. Two pressure sensors were used to measure the pressure drop. Top pressure sensor was located at distance of 32 cm from the top. The distance between the two pressure sensors was 0.5 m. Glass beads were supported at the bottom by a stainless steel plate having 3 mm holes with 3 mm triangular pitch. Liquid was collected in a cup at the bottom of the column after gas was separated from the side outlet. Cup was made-up of aluminum material with 5 cm inner diameter. Conductivity probe was hold inside the cup to measure the tracer concentration. Salt solution (concentration 50 gm/lit) was used as a tracer. Tracer was injected with the help of a syringe placed at a distance of 16.6 cm from the top of the packed bed. The needle of the syringe was extended up to the bed center. For each experiment, 20 ml of tracer was injected. Out-put signals of conductivity probe as well as pressure probes were acquired with 16 bit PCMCIA card, a laptop computer and dAtagate software (of nCode Inc., UK).

Operating Parameters and Procedure

Experiments were performed for two particle sizes: spherical particles of 3 mm and 6 mm diameter. Pressure drop, dynamic liquid hold-up and tracer concentration at the outlet were measured for the range of gas (0-0.44 m/s) and liquid (3-10 mm/sec) superficial velocities. Before starting of each experiment, air passed through column for 5-6 hrs so that complete dry bed conditions are achieved. For non-wetted bed, liquid flow rate was gradually increased and pressure drop and dynamic liquid hold-up were measured. Dynamic liquid hold-up was measured by switching off inlet air and liquid flows and by collecting the drained liquid. At steady state, 20 ml of tracer was injected through the syringe. The injection time was approximately 3-4 sec. The conductivity probe signal was collected online with data acquisition frequency of 100 Hz. Data was acquired for 200 sec.

CFD Model for Trickle Bed Reactor

In trickle bed reactor, gas is a continuous phase, while liquid is a semi-continuous phase. In this work, a CFD model based on Eularian-Eularian framework model was developed to simulate the gas-liquid flow in trickle bed reactor. Radial as well as axial porosity variation in the packed bed was considered in the model. Mixing and dispersion of liquid phase tracers were simulated using the CFD model. The details of model equations are discussed below.

Representing Non-uniform Porosity Distribution

Previous experimental studies have shown that for a randomly packed bed, porosity is higher near the vicinity of wall and it fluctuates significantly in the near wall region (of width of about 4 to 5 particle diameters). The magnitude of fluctuations is a strong function of a ratio of column diameter to particle diameter (for $D/d_p > 15$, fluctuations are within 1% whereas for lower values of D/d_p, fluctuations may rise up to 30%). Mueller (1991) has proposed a correlation for radial variation of axially averaged porosity as a function of column diameter, particle diameter and average porosity (ϵ_B) as:

$$\epsilon(r) = \epsilon_B + (1-\epsilon_B) J_o(ar^*) e^{-br}$$

where,

$$a = 8.243 - \frac{12.98}{(D/d_p - 3.156)} \text{ for } 2.61 \le D/d_p \le 13.0$$

$$a = 7.383 - \frac{2.932}{(D/d_p - 9.864)} \text{ for } 13.0 \le D/d_p \qquad (1)$$

$$b = 0.304 - \frac{0.724}{D/d_p}$$

$r^* = r/D$ and J_o is zeroth order Bessel Function

This equation was used in the computational model to prescribe the radial variation of axially averaged bed porosity. Additional assumptions about how the porosity varies in axial direction are however needed to complete the prescription of bed porosity. Jiang et al. (2001) have shown that axial porosity variation is close to Gaussian distribution function, and this was followed in our work. Thus, for any radial position, axially averaged porosity was calculated using Equation (1). Porosity variation along the axial direction (as well as in tangential direction in 3-D case) was specified using this average value and assumption of Gaussian distribution with specified standard deviation. The value of standard deviation was taken as 5% unless mentioned otherwise.

Model Equations

Flow in trickle bed reactor was simulated using multi-fluid model. Governing equations are given below.

Mass Balance Equation:

$$\frac{\partial \varepsilon_K \rho_K}{\partial t} + \nabla \cdot \varepsilon_K \rho_K U_K = 0 \tag{2}$$

Momentum Balance Equation:

$$\frac{\partial(\varepsilon_K \rho_K U_K)}{\partial t} + \nabla \cdot (\varepsilon_K \rho_K U_K U_K) = -\varepsilon_K \nabla P + \nabla \cdot (\varepsilon_K \mu \nabla U) + \varepsilon_K \rho_K g + F_{K,R}(U_k - U_R) \tag{3}$$

Where, ε_k represents the volume fraction of each phase, ρ_k is the density of k^{th} phase. U_k is the velocity of k^{th} phase. P is a mean pressure shared by all the phases present in the system. $F_{K,R}$ is inter-phase momentum exchange terms. It is assumed that there is no inter-phase mass transfer. The mass balance Equation (2), therefore, does not have any source term on the right hand side. The left hand side of Equation (3) represents the rate of change of momentum for k^{th} phase. The right hand side represents pressure forces, gravitational acceleration, average shear stresses and inter-phase momentum exchange. Inter-phase coupling terms $F_{K,R}$ (given here by Equations (4) to (6) proposed by Attou and Ferschneider (2000) were used in the present work.

Gas-Liquid Momentum Exchange Term:

$$F_{GL} = \varepsilon_G \left(\frac{E_1 \mu_G (1-\varepsilon_G)^2}{\varepsilon_G{}^2 d_p^2} \left[\frac{\varepsilon_S}{(1-\varepsilon_G)} \right]^{0.667} + \frac{E_2 \rho_G (U_G - U_L)(1-\varepsilon_G)}{\varepsilon_G d_p} \left[\frac{\varepsilon_S}{(1-\varepsilon_G)} \right]^{0.333} \right) \tag{4}$$

Gas-Solid Momentum Exchange Term:

$$F_{GS} = \varepsilon_G \left(\frac{E_1 \mu_G (1-\varepsilon_G)^2}{\varepsilon_G{}^2 d_p^2} \left[\frac{\varepsilon_S}{(1-\varepsilon_G)} \right]^{0.667} + \frac{E_2 \rho_G U_G (1-\varepsilon_G)}{\varepsilon_G d_p} \left[\frac{\varepsilon_S}{(1-\varepsilon_G)} \right]^{0.333} \right) \tag{5}$$

Liquid-Solid Momentum Exchange Term:

$$F_{LS} = \varepsilon_L \left(\frac{E_1 \mu_L \varepsilon_s{}^2}{\varepsilon_L{}^2 d_p^2} + \frac{E_2 \rho_L U_G \varepsilon_S}{\varepsilon_L d_p} \right) \tag{6}$$

It must be noted that a pressure shared by all the phases is used in momentum balance equation (Equation 3). However, the pressures in gas and liquid phases at the gas–liquid are different due to surface tension. The difference is called as capillary pressure and is given by:

$$P_c = P_G - P_L = 2\sigma \left(\frac{1}{d_1} - \frac{1}{d_2} \right) \tag{7}$$

where, d_1 and d_2 are the maximum and minimum diameter of the sphere with liquid film formed by the flowing liquid. More details of relating d_1 and d_2 to particle diameter, porosity and the minimum equivalent diameter of the area between three particles in contact are given in Attou and Ferschneider (2000). Capillary pressure affects the liquid distribution and may set-up gradients of liquid hold-up within the packed bed.

The order of magnitude analysis indicates that the magnitude of the capillary forces is rather small compared to the magnitudes of inter-phase drag forces. Attou and Ferschneider (2000) have obtained the following expression for the capillary pressure term based on geometric estimates of d_1 and d_2 and with empirical factor F to account for high-pressure operations as:

$$P_g - P_L = 2\sigma \left(\frac{1-\varepsilon}{1-\varepsilon_G} \right)^{0.333} \left(\frac{5.416}{d_p} \right) F\left(\frac{\rho_G}{\rho_L} \right) \tag{8}$$

where,

$$F\left(\frac{\rho_G}{\rho_L} \right) = 1 + 88.1 \frac{\rho_G}{\rho_L} \; for \; \frac{\rho_G}{\rho_L} < 0.025 \tag{9}$$

It must be noted here that in trickle beds, the pressure drop required to maintain specified gas and liquid throughputs is history dependent. Pressure drop at any specific liquid velocity measured with increasing liquid velocity is more than that measured with decreasing liquid velocity (see for example, Szady and Sundaresan, 1991). Capillary phenomenon is one of the contributing factors of this observation. Jiang et al. (2001) have attempted to simulate this phenomenon by introducing an empirical factor, f, related to the degree of wetting in their capillary pressure formulation as:

$$P_G - P_L = (1-f) P_c \tag{10}$$

For pre-wetted bed, f is set to one, implying zero capillary pressure. For non-wetted bed, f is set to zero (Jiang et al., 2001). As will be seen later in this work, the difference in the predicted pressure drop with and without considering capillary terms is not as high as the observed magnitude of the hysteresis of the pressure drop. In the present work, therefore, all the simulations were carried out with setting f equal to zero unless otherwise noted.

For incorporating the capillary pressure in the CFD model, gradients of capillary pressure must be formulated as:

$$\frac{\partial P_G}{\partial z} - \frac{\partial P_L}{\partial z} = \frac{2}{3}\sigma \frac{5.416}{d_p}\left(\frac{\epsilon_s}{1-\epsilon_G}\right)^{-2/3} \left(\left(\frac{1}{1-\epsilon_G}\right)\frac{\partial \epsilon_s}{\partial z} + \left(\frac{\epsilon_s}{(1-\epsilon_G)^2}\right)\frac{\partial \epsilon_G}{\partial z}\right) F\left(\frac{\rho_G}{\rho_L}\right) \quad (11)$$

The right hand side of the Equation (11) was added to the right hand side of liquid phase momentum equations to incorporate the capillary pressure terms.

The following scalar transport equation was included to simulate mixing of tracer in trickle bed reactors:

$$\frac{\partial \varepsilon_K \rho_K C_i}{\partial t} + \nabla \cdot \varepsilon_K \rho_K U_K C_i = -\nabla \cdot \left(\varepsilon_K \rho_K D_{i.m} \nabla C_i\right) + S_i \quad (12)$$

Tracer transport equations were solved simultaneously with the momentum transport equations.

Boundary Conditions and Numerical Solution

Flow in trickle bed reactors was simulated by considering (1) axis-symmetric (two-dimensional), and (2) full three dimensional domain. For two-dimensional domain, 150 cells in axial direction and 20 cells in radial direction were used (see Figure 2a). For three-dimensional domain, 100 cells in axial direction and 20 cells in radial and tangential direction were used. For both the cases, grid sizes were found to be adequate, as further increase in number of grids did not significantly affect the predicted flow results. The model equations described earlier were solved using FLUENT 4.5 (Fluent. Inc., USA). For 2-D model, axis-symmetric boundary condition was implemented where solution was assumed to be symmetric in tangential direction. Porosity for each cell was assigned with the help of a user defined subroutine. Flat velocity profile was implemented for gas and liquid phases as inlet boundary condition. No slip boundary condition was used for all the impermeable walls. Momentum exchange coefficients and capillary pressure terms were implemented using user-defined routines. Velocity of the solid phase was set to zero. Unsteady simulations were carried out with the time step of 0.01 s.

First gas–liquid flow through packed bed was simulated without considering the tracer in flow. For pre-wetted (without capillary term) and for non-wetted (capillary term) simulations were carried out. Typical variation in liquid hold-up in bed for these two cases is shown in Figure 2b. For simulations of tracer mixing, a tracer inlet was defined at appropriate location (16.6 cm from top of the column; see Figure 2a). While carrying out experiments, tracer was injected with a needle. However, due to the constraints imposed by grid size and numerical stability, the modeled tracer inlet was considered as much larger than the needle size (~0.026 m). Scalar and momentum transport equations were solved simultaneously. After the addition of 20 ml of tracer, tracer input was stopped. Typical predicted tracer dispersion after 2 seconds is shown in Figure 2c. Tracer concentration were averaged at the bottom cells and recorded for each time step.

Results and Discussion

Pressure Drop/Liquid Hold-up

The pressure drop in trickle bed reactors were measured for non-wetted beds as well as for pre-wetted bed at different

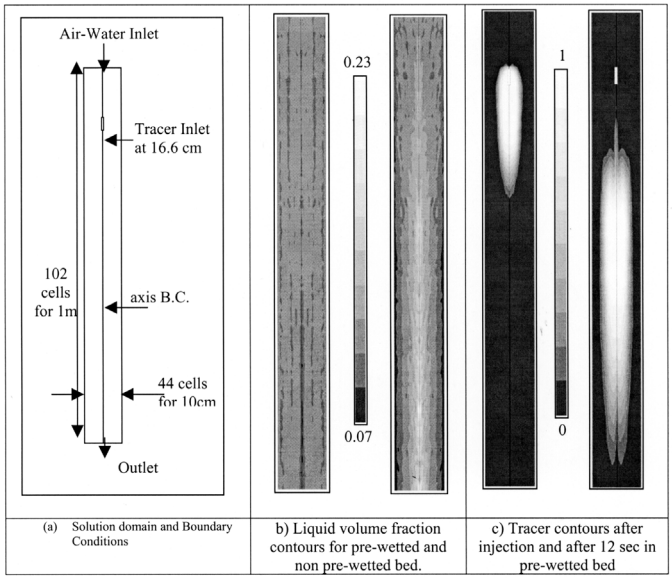

Figure 2. Solution domain, liquid volume fraction and tracer mass fraction contours for trickle bed reactor. Operating conditions: V_L = 2kg/m2s, V_G = 0.22m/s, d_p = 3mm, Std. Dev. = 5%, E_1 = 180, E_2 = 1.75.

operating conditions. The measured pressure drop values for different liquid velocity at V_G = 0.22m/sec are shown in Figure 3a. It can be seen that the pressure drop variation with liquid velocity is very different for the pre wetted and the dry (non-prewetted) bed. Similar results were reported earlier by Sundaresan et al. (1992) and Ravindra et al. (1997). The magnitude of difference between pressure drop per unit length for pre-wetted bed and non pre-wetted bed depends upon how well the bed was dried before starting the experiments. From Figure 3(a), it was observed that for dry bed, pressure drop remained as low as 2.3 kPa/m till V_L = 9 kg/m^{2}s and then suddenly increased almost 5 to 6 times with further increase in liquid velocity (beyond 10 kg/m^{2}s). For non pre-wetted bed, liquid flows through confined region of the bed, and hence the pressure drop is low. As the liquid velocity increases beyond 10 kg/m^2·s, liquid begins to disperse throughout the bed and wets the bed. Air-water interaction increases under wetted conditions and hence, pressure drop suddenly increases when wetted conditions are realized in the initially dry bed. Measurements with larger particles (6 mm) indicated that the magnitude of hysteresis in the pressure drop obtained for bed with 6 mm particles is lower than that observed with the 3 mm particles (see Figure 3a). This result implies that the effect of capillary pressure is less dominant in 6 mm particle compared with the 3 mm particle bed.

The dynamic liquid hold-up was measured using drainage method. Hysterisis was also observed in the measured values of dynamic liquid hold-up (see Figure 3b). However, the magnitude of hysteresis in dynamic liquid hold-up was much lower than that observed in the case of pressure drop. Static liquid hold-up (which is a function of the particle diameter and properties of liquid), could not be measured and was estimated from the correlation given by Saez and Carbonell (1985) as:

$$\varepsilon_{LS} = \frac{1}{20 + 0.9\ddot{E}o} \quad (13)$$

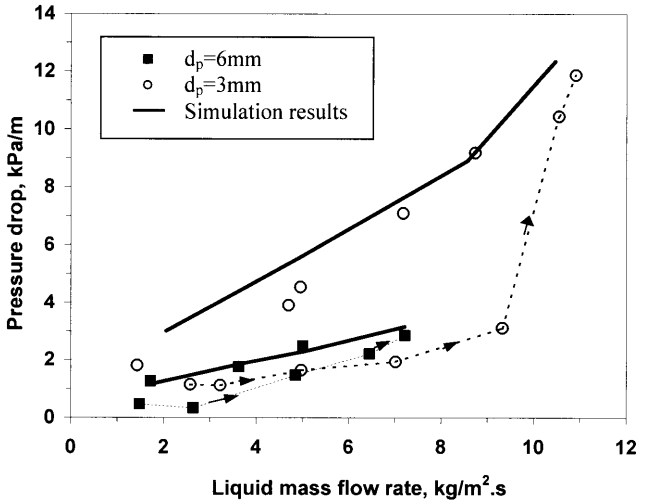

Figure 3a. Comparison of pressure-drop in TBR with simulation results. Operating conditions: V_G = 0.22m/s, Std. Dev. = 5%.

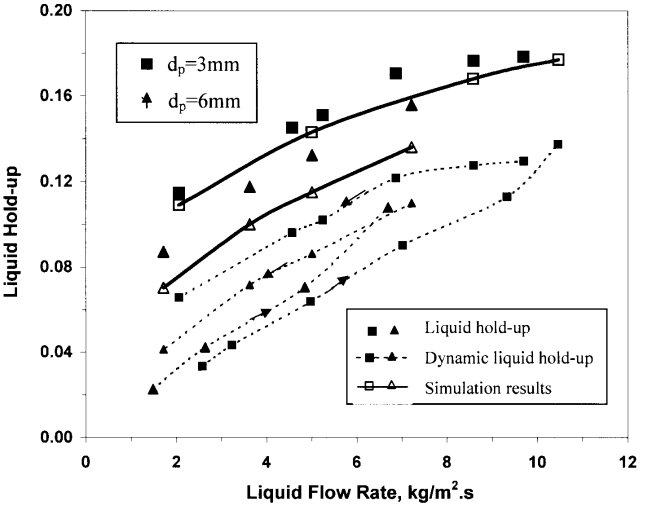

Figure 3b. Comparison of liquid hold-up in TBR with simulation results. Operating conditions: V_G = 0.22m/s, Std. Dev. = 5%, E_1 = 180, E_2 = 1.75.

where,

$$\ddot{E}o = \frac{\rho_L g d_p^2 \varepsilon^2}{\sigma_L\left(1-\varepsilon^2\right)^2} \tag{14}$$

The total liquid hold-up was obtained by summing the measured dynamic hold-up and the estimated static liquid hold-up.

Simulations were carried out for 3 mm and 6 mm particle diameter. The predicted values of pressure drop and liquid hold-up were compared with experimental data. The values of Ergun's constants E_1 and E_2 were set to 180 and 1.75 for 3 mm diameter particle bed and 500 and 2.4 for 6 mm diameter particle bed respectively. Similar values were used to the particles of 3 mm and 6 mm in the previous studies (see a review of Holub et al., 1992). Simulations were carried out with and with out considering the capillary pressure terms. Figure 2b shows the contours of the liquid distribution in bed simulated for pre-wetted bed and non pre-wetted bed. Comparison of simulated results and experimental data is shown in Figure 3a and 3b. Unlike experimental data, the simulated results showed much less difference in the pressure drop values obtained for pre-wetted bed and non pre-wetted bed (~200 Pa/m). The reasons for this discrepancy are not obvious and need further studies on capillary, wetting and inter-phase closure models. Simulated results of pre-wetted bed were found to be in good agreement with experimental data of pressure drop and total liquid hold-up. The CFD model was therefore extended to simulate mixing and residence time distribution in TBR.

Experimental Data of Residence Time Distribution

Exit age distribution shows the time history of the tracer flow path through the packed bed. Liquid flow in a packed bed was affected by severe parameters like liquid distributor, bed interstitial geometry, properties of liquid and capillarity. From the outlet tracer concentration, exit age distribution was calculated as:

$$E(t) = \frac{C_i}{\int_0^\infty C_i dt} \tag{15}$$

Exit age distribution $E(t)$ of tracer in a trickle bed reactor was measured at different operating conditions and plotted as a function of time. Measured values of $E(t)$ for 3 mm particle are shown in Figure 4. At low liquid flow rates (2-3 kg/m^2·s), large variation in $E(t)$ response curve was observed for pre-wetted and non pre-wetted bed. Liquid is more dispersed for pre-wetted bed than non pre-wetted bed (Figure 4). At low liquid flow rate, in non pre-wetted bed, liquid flow was restricted to confined region within the bed and hence exit age distribution shows dominant plug flow characteristics. As liquid flow rate increases, the observed difference in the exit age distributions for pre wetted and non pre-wetted conditions reduces. At high liquid flow rates (10kg/m^{2}s), where capillary pressure effect is negligible, $E(t)$ variation is almost path independent. For 6 mm particle bed, at low liquid flow rates liquid dispersion was less compared to 3 mm particle bed. Similar to the pressure drop hysteresis, the difference in the exit age distributions for pre-wetted and non pre-wetted was less for 6 mm particle bed. Effect of capillary pressure is in 3 mm particle bed is stronger than 6 mm particle bed.

CFD Simulations of Tracer Mixing in Trickle Bed

Preliminary simulations were carried out to examine influence of liquid velocity, bed heterogeneity and capillary pressure on liquid dispersion and RTD. Results of these numerical experiments are discussed in the following before the simulated RTD results are compared with the experimental data.

Effect of Bed Heterogeneity on RTD

To understand influence of bed heterogeneity on liquid tracer response in trickle beds, simulations were carried out for beds with different porosity: (a) uniform porosity, (b) radially varying

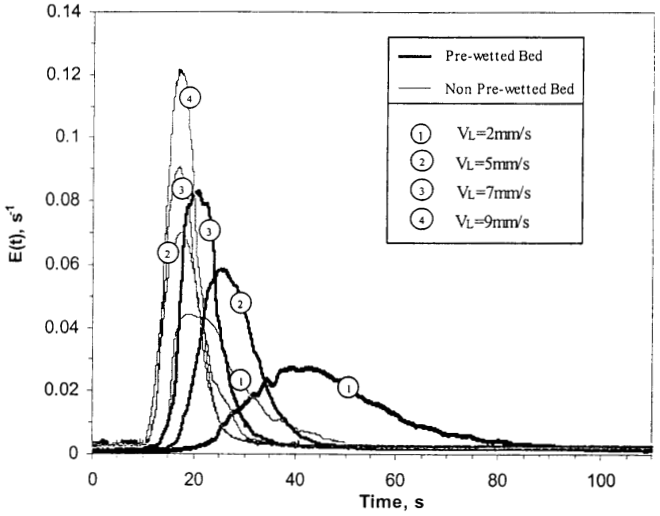

Figure 4. Measured residence time distribution in trickle bed reactor for d_p = 3mm and V_G = 0.22m/s.

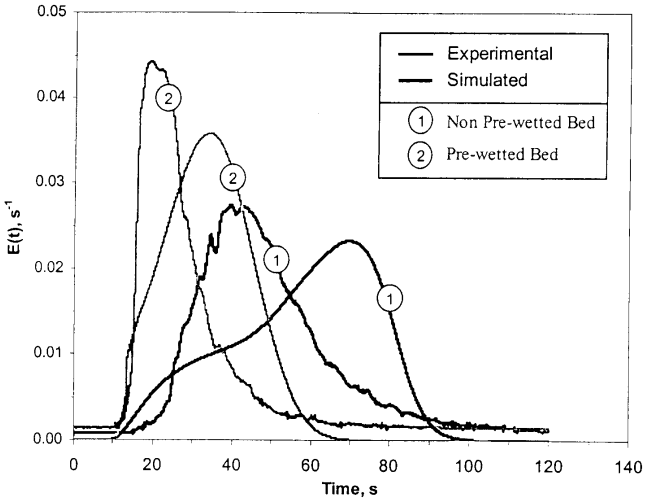

Figure 5. *Comparison of experimental RTD response with simulated results. Operating conditions: V_L = 2kg/m2s, V_G = 0.22m/s, Std. Dev. = 5%, dp = 3mm, E_1 = 180, E_2 = 1.75.*

porosity according to Equation (1c) randomized bed porosity with 5% standard deviation super imposed on Equation (1d) randomized bed porosity with 10% standard deviation super imposed on Equation (1). For case b, transverse velocity component is almost absent and liquid flows vertically downwards. As randomness in porosity increases (std. dev. 5 and 10%), magnitude of liquid phase velocity in transverse direction increases. Tracer simulations of these cases were carried out and simulated RTD response at different bed heterogeneity with the experimental data was compared. It was observed that without inclusion of random porosity in the computational model, simulated RTD shows qualitatively different behavior than that observed in experiments. It is, however, difficult to experimentally measure the extent of bed heterogeneity. The experimentally measured tracer RTD curve falls in between simulated curves obtained with 5% and 10% standard deviation. In absence of quantitative measurement of bed heterogeneity of the trickle bed used in the experiments, all the subsequent simulations were carried out by considering 5% standard deviation.

Effect of Capillarity on Tracer Response

Experimental data of pressure drop and tracer response show that capillary pressure plays a major role in liquid distribution and hydrodynamics of the trickle bed. Most of the industrial trickle bed reactors are operates at low liquid flow rate where non-wetting conditions are most likely to occur. To understand influence of pre-wetting on RTD, simulations of tracer mixing were carried out at pre-wetted conditions (without considering the capillary pressure in the model) and at non pre-wetted bed conditions (with considering the capillary pressure). The simulated results are shown in Figure 2b for 3 mm particle size. It can be seen that liquid flow is confined to the central region for the case of non pre-wetted bed; unlike the pre-wetted bed, where it is uniformly distributed. Exit age distributions for 3 mm and 6 mm particle beds under pre-wetted and non-prewetted conditions were compared with the experimental data in Figures 5 and 6 respectively. It can be seen that agreement between simulated results and experimental data is much better for the bed with 6 mm particles than that with 3 mm particles. Capillarity effect is dominant for the bed with 3 mm particles.

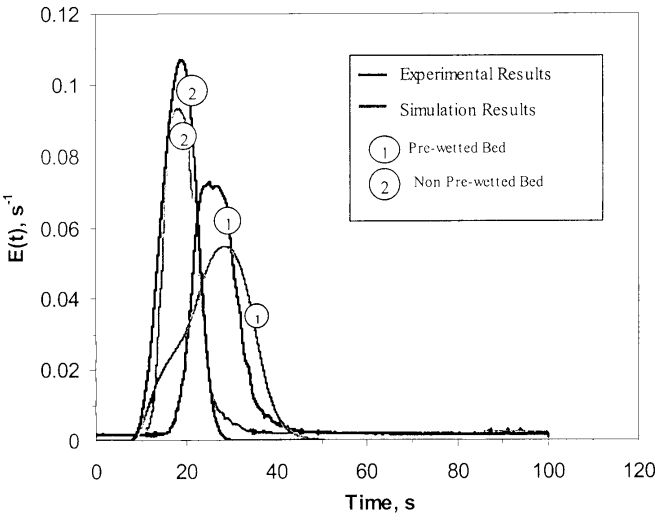

Figure 6. Comparison of experimental RTD response with simulated results. Operating conditions: V_L = 1.72kg/m2s, V_G = 0.22m/s, Std. Dev. = 5%, *dp* = 6mm, E_1 = 500, E_2 = 3.4.

The current models used for capillary effect appear to be unable to capture the microscopic details of wetting and the effect on pressure drop and mixing. Another possible reason for the observed discrepancy may be an inadequate accuracy of representing local variation of bed porosity. It should be noted that while assigning the variation of bed porosity, simulations 5% standard deviation was assumed for both, 3 mm and 6 mm particle beds. Particle diameter is likely to affect the degree of heterogeneity of the bed. Unfortunately, quantitative information about such influence is not available at present. Despite some of these issues, it may be said that the agreement between simulated and experimental results is encouraging. The model was therefore extended to examine the possibility of simulating flow and mixing in TBR with non-uniform inlet.

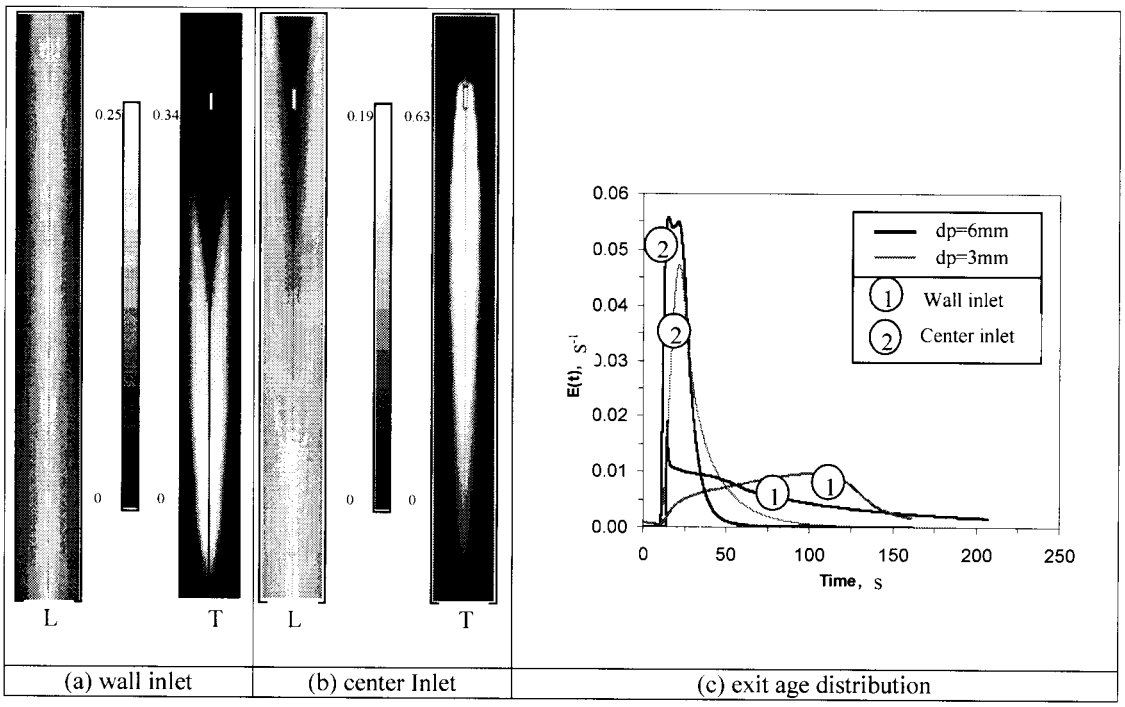

Figure 7. Liquid volume fraction and tracer mass fraction for bed with center and wall inlets. L = Liquid Hold-up contours, T = Tracer dispersion contours. Operating conditions: V_L = 2kg/m2s, V_G = 0.22m/s, d_p = 3mm, Std. Dev. = 5%, E_1 = 180, E_2 = 1.75.

Flow Mal-distribution in TBR

Liquid flow mal-distribution may occur in trickle bed reactors due to several possible reasons including non-uniform liquid distribution at the inlet, local porosity distribution and capillarity action. Previous attempts to study liquid mal-distribution were mainly experimental (Sapre et al., 1990). Recently, Song et al. (1998) used CFD model to examine mixing in packed beds (with Pall rings). In this work, with the help of CFD model, now it is possible to simulate the tracer path in non-uniform liquid inlet operating condition. As discussed before, the present model incorporates random porosity distribution and capillary terms. For non-uniform liquid inlet, it may be necessary to consider full three-dimensional solution domain. However, before we discuss results obtained with such 3D cases, results of some numerical experiments carried out with two-dimensional domain are discussed to bring out key features of mal-distribution.

Two cases were considered: Case a- liquid enters through an annular region ($r/R > 0.75$) near the wall of the column and Case b- liquid enters through the central region ($r/R < 0.5$) of the column. Simulations were carried out for non pre-wetted bed at liquid flow rate of 2 kg/m^2·s. Simulated results for the 3 mm particle diameter are shown in Figure 7. It can be observed that liquid distribution becomes more uniform when liquid is introduced through the central region (Figure 7a(L)), compared to the case with wall inlet (Figure 7b(L)). The extent of non-uniformity was found to be larger in the case of 6 mm particle compared to that of 3 mm particle. Contours of the tracer mass fraction at 10 sec after injection are also shown in Figure 7a-b (T). For center inlet flow condition, tracer flows faster through the bed showing plug flow like behavior for both the cases, i.e., 3 mm and 6 mm particle sizes. For liquid inlet near wall, tracer contours show prolonged tail since the tracer injection location was in stagnant zone of the bed. Figure 7c shows corresponding exit age distribution curves. It can be seen that mean residence time of tracer for the case of liquid entering through the center is much less than that for the case with the wall inlet. In actual practice, non-symmetric liquid distribution often occurs and hence, it was decided to carry out specific experiments to understand influence of non-uniform liquid inlet.

Rather than selecting symmetric central or annular region, experiments were deliberately carried out with asymmetric liquid inlet. Experiments were carried out by allowing liquid to pass through 25% area of the total inlet (Figure 8a). Experiments were carried out for two tracer injection locations located at 16.6 cm from the top: one at the middle of the inlet region and the second at the column center (Figure 8a). Experimental RTD was measured for both the locations with pre-wetted as well as non pre-wetted bed conditions. Experimental RTD responses at different injection locations are shown in Figure 9. It can be seen that, for non pre-wetted bed, mean residence time obtained with in-stream injection (location A) is close to plug flow behaviour. This indicates poor liquid dispersion in radial direction due to non pre-wetted condition. Such poor dispersion in radial direction causes a prolonged tail in RTD for the case with off-stream (location B) tracer injection (see Figure 9). Contrary to this, for the pre-wetted bed, the injected tracer quickly spreads in radial direction and therefore there is not a significant difference in the tracer response for the pre-wetted and non pre-wetted bed.

It is essential to consider full three-dimensional solution domain to simulate tracer mixing with asymmetric liquid inlet. For the 3D solution domain, random porosity variations along axial and tangential direction were imposed on axially averaged porosity given by Equation (1). Figure 8a shows the body fitted grid used for the column. Few highly skewed cells were omitted

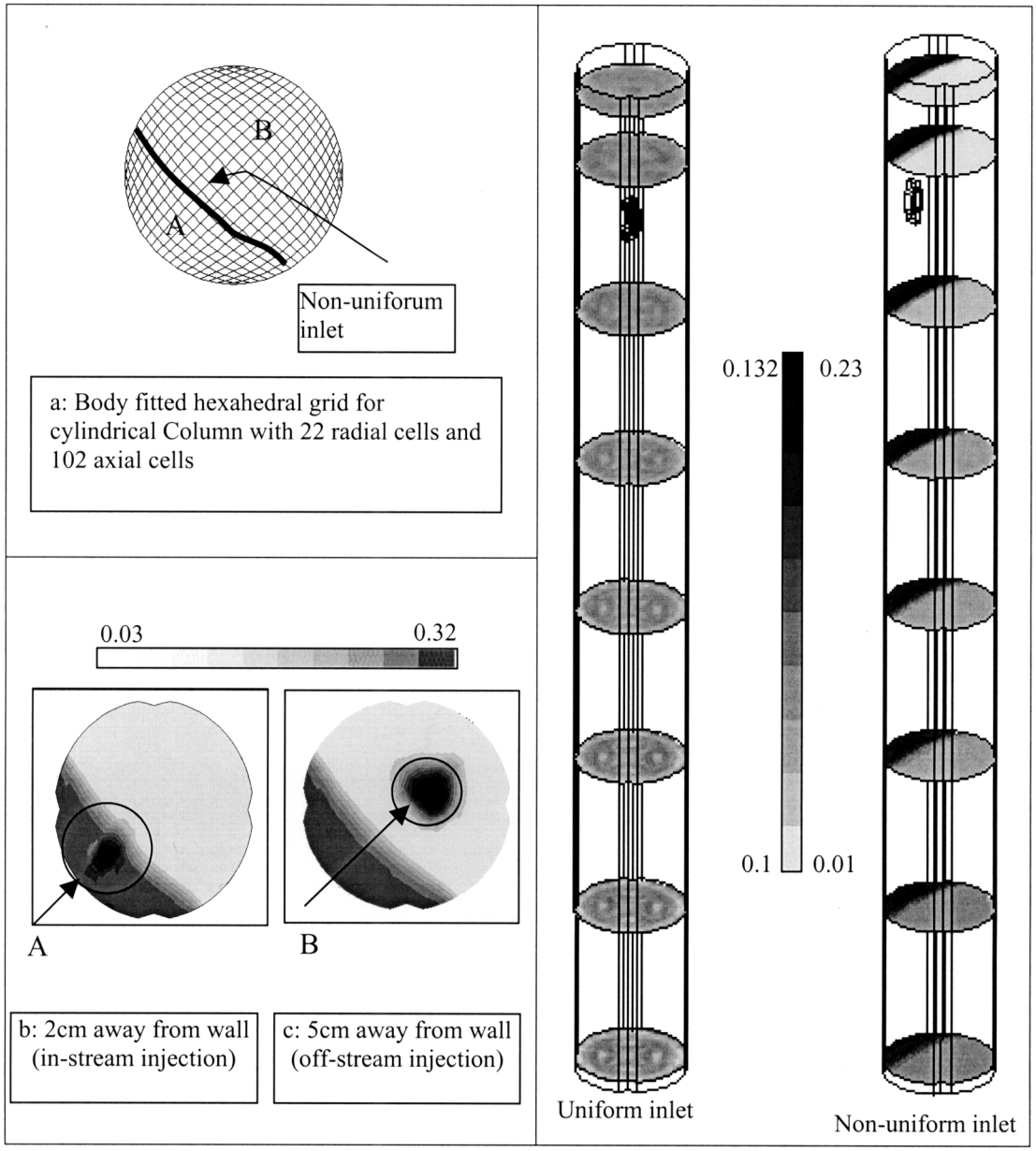

Figure 8. 3-D column grid, tracer injection points and liquid volume fraction contours in uniform and non-uniform inlet conditions. Operating conditions: V_L = 2kg/m2s, V_G = 0.22m/s, d_p = 3mm, Std. Dev. = 5%, E_1 = 180, E_2 = 1.75.

from the domain to avoid the numerical instability. Simulations were carried out for two cases: uniform inlet and non-uniform inlet (liquid entering through 25% of the column area) for the liquid phase. Uniform air inlet was specified for both of these cases. Tracer mixing simulations were carried out for two-tracer location used in the experiments (locations A and B shown in Figure 8a). Contours of predicted tracer mass fraction for the two cases are shown in Figures 8b and 8c. Corresponding predicted distributions of liquid hold-up are shown in Figure 8(d). Since the simulations were carried out for pre-wetted bed, non-uniformities in liquid distribution reduce along the length of the column. However, significant non-uniformities were still found to be present even at the column outlet.

The simulated RTD curves for the two tracer injection locations for pre-wetted bed case are shown in Figure 10. Experimental data of non-uniform liquid inlet (see Figure 9) shows that pre-wetted bed condition improves the liquid distribution considerably. Unlike the experimental results, the simulated results show long tails in the predicted tracer response. These results indicate that the model is predicting very poor radial dispersion than the actual dispersion occurring in the TBR. Poorer radial mixing is very severe for the case of off-stream injection, leading to extremely long tail. For this case, the simulations were stopped before the entire tracer came out of the TBR. Inadequate accounting of the variation of bed porosity and the wetting and capillary processes are the most likely reasons for the observed under-prediction of radial dispersion. Further studies on these aspects, especially the role of gradients of liquid volume fraction and radial dispersion of tracer in liquid phase, need to be carried out. The models and results presented here would be useful for such further studies on radial mixing of tracer in trickle beds.

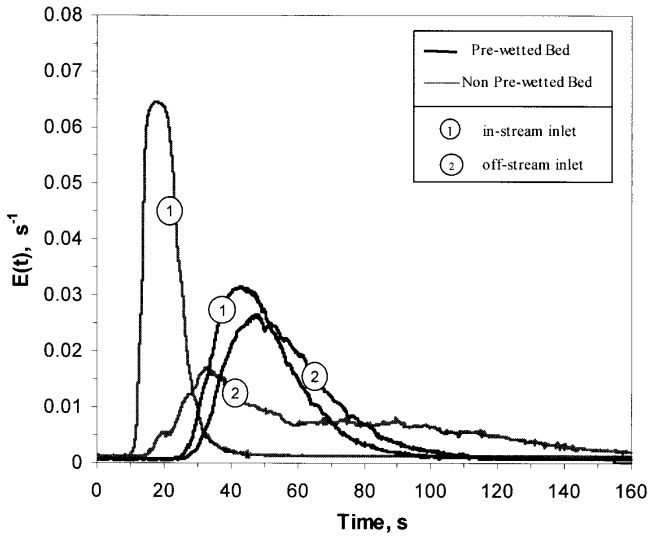

Figure 9. Experimental RTD response in pre-wetted and non pre-wetted bed for non-uniform inlet conditions. Operating conditions: V_L = 2kg/m2s, V_G = 0.22m/s, d_p = 3mm, Std. Dev. = 5%, E_1 = 180, E_2 = 1.75.

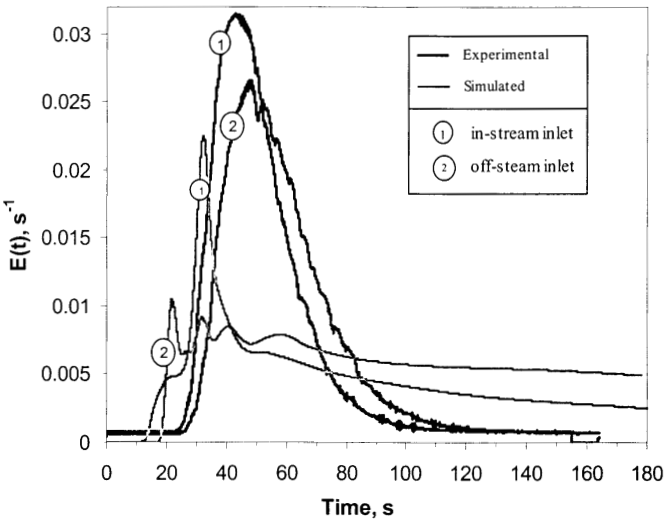

Figure 10. Comparison of experimental and simulated RTD with non-uniform inlet. Operating conditions: V_L = 2kg/m2s, V_G = 0.22m/s, d_p = 3mm, Std. Dev. = 5%, E_1 = 180, E_2 = 1.75.

Conclusion

Liquid distribution and mixing (residence time distribution) in trickle bed reactors was studied using experiments and computational flow model. Different modeling issues, such as porosity distribution within the bed, capillary pressure model and grid size, were discussed. The present study suggests that capillary pressure (or wetting) has dominant effect on liquid distribution than the porosity distribution. Though current capillary pressure models are unable to quantitatively predict hysteresis in pressure drop, CFD model gives encouraging trends for tracer residence time distribution and liquid mixing in pre-wetted and non pre-wetted beds. The CFD model was also able to capture the influence of non-uniform and asymmetric liquid inlet. For asymmetric liquid inlet, simulation results show under prediction of dispersion. Inadequate accounting of the variation of bed porosity and the wetting and capillary processes are the most likely reasons for the observed under-prediction of radial dispersion. The models and results presented here would be useful for further studies on radial mixing of tracer in trickle beds.

Nomenclature

C_i	tracer concentration, (kg/m^3)
d_1, d_2	max and min diameter of liquid film flowing over sphere, (m)
D	diameter of bed, (m)
$D_{i,m}$	molecular diffusivity, (m^2/s)
d_p	particle diameter, (m)
$E(t)$	exit age distribution, (s^{-1})
E_1, E_2	Ergun's constants
F	moment exchange coefficients, (kg/m^3·s)
f	wetting factor
g	acceleration due to gravity, (m/s^2)
J_o	zeroth order Bessel function
L	length of the bed
P	pressure, (N/m^2)
$(\Delta P/L)$	pressure drop per unit length, (N/m^3)
Si	source term, (kg/m^2·s)
r	radius of column
t	time, (s)
U	cell velocity, (m/s)
V_G	gas mass velocity, (kg/m^2/s)
V_L	liquid mass velocity, (kg/m^2/s)

Greek Symbols

β	liquid saturation
ε	bed porosity
ε_P	porosity in the jth cell
ε_B	average porosity of bed
ε_k	volume fraction of k^{th} phase
$\varepsilon(r)$	axially averaged bed porosity at radius r
ε_{LS}	static liquid hold-up
μ_k	viscosity of phase k in the bed, (Pa.s)
ρ_k	density of k phase, (g/mL)
σ	surface tension, (N/m)

Subscript

G	gas phase
k	phase
L	liquid phase
R	phase other than k

References

Attou, A. and G. Ferschneider, "A Two-fluid Hydrodynamic Model for the Transition between Trickle and Pulse Flow in a Cocurrent Gas-liquid Packed-bed Reactor", Chem. Eng. Sci., **55**, 491–511 (2000).

Oliveros, G. and J.M. Smith, "Dynamic Studies of Dispersion and Channeling in Fixed Beds" AIChE J. **28**, 751–759 (1982).

Gulijk, C.V., "Using Computational Fluid Dynamics to Calculate Transversal Dispersion in a Structured Packed Bed" Comp. Chem Eng. **22**, 5767–5770 (1998).

Hanratty, P.J. and M.P. Dudukovic, "Detection of Flow Maldistribution in Trickle-bed Reactors via Tracers" Chem. Eng. Sci. **47**, 3003–3014 (1992).

Holub, R.A., M.P. Dudukovic and P.A. Ramachandran, "A Phenomenological Model for Pressure Drop, Liquid Holdup, and Flow Regime Transition in Gas-liquid Trickle Flow" Chem. Eng. Sci. **47**, 2343–2348 (1992).

Jiang, Y., M.R. Khadilkar, M. Al-Dahhan and M.P. Dudukovic., "CFD of Multiphase Flow in Packed Bed Reactors: I. Modeling Issues", AIChE J. **48**, 701–715 (2002).

Mueller, G.E., "Prediction of Radial Porosity Distribution in Randomly Packed Fixed Beds of Uniformly Sized Spheres in Cylindrical Containers" Chem. Eng. Sci. **46**, 706–708 (1991).

Ramachandran, P A. and J.M. Smith, "Dynamic Behavior of Trickle Bed Reactor" Chem. Eng. Sci. **34**, 75–91 (1978).

Ranade V.V., "Computational Flow Modeling for Chemical Reactor Engineering", Academic Press, London, UK (2002).

Ranade, V.V., P.R. Gunjal and R.V. Chaudhari, "Estimation of Frictional Pressure Drop and Supported Liquid Saturation in Trickle Bed Reactors Using CFD Models", submitted to Chem. Eng. Res. and Des. (2002).

Ravindra, P. V., D.P. Rao and M.S. Rao, "Liquid Flow Texture in Trickle Bed Reactors: an Experimental Study" Ind. Eng. Chem. Res. **36**, 5133–5145 (1997).

Robinson B.A and J.W. Tester, "Characterization of Flow Mal-distribution Using Inlet-Outlet Tracer Techniques: An Application of Internal Residence Time Distributions", Chem. Eng. Sci. **41**. 469–483 (1986).

Sapre, A.V., D.H. Anderson and F.J. Krambeck, "Heater Probe Technique to Measure Flow Mal-distribution in Large Scale Trickle-bed Reactors". Chem. Eng. Sci. **45**, 2263–2268, (1990).

Schwartz, J.G., E. Weger and M.P. Dudukovic, "A New Tracer Method for the Determination of Liquid-solid Contacting Efficiency in Trickle Bed Reactors" AIChE. J. **22**, 953–960 (1976).

Song M., F.H. Yin, K. Nandakumar and K.T. Chuang, " A Three-dimensional Model for Simulating the Mal-distribution of Liquid Flow in Random Packed Beds" Can. J. Chem. Eng. **76**, 161–166 (1998).

Specchia, V. and G. Baldi, Pressure Drop and Liquid Holdup for Two-phase Concurrent Flow in Packed Beds. Chem. Eng. Sci. **32**, 515–523 (1977).

Szady, M.J. and S. Sundaresan, "Effect of Bboundaries on Trickle-bed Hydrodynamics" AIChE J. **37**, 1237–1241 (1991).

Manuscript received November 22, 2002; revised manuscript received April 25, 2003; accepted for publication June 6, 2003.